 CMC, vol.8, no.1, pp.23-31, 2008

Green's Function for Multilayers with Interfacial Membrane and Flexural Rigidities[1]

B. Yang[2] and V. K. Tewary[3]

Abstract: A three-dimensional Green's function for a material system consisting of anisotropic and linearly elastic planar multilayers with interfacial membrane and flexural rigidities has been derived. The Stroh formalism and two-dimensional Fourier transforms are applied to derive the general solution for each homogeneous layer. The Green's function for the multilayers is then solved by imposing the surface boundary condition, the interfacial displacement continuity condition, and the interfacial traction discontinuity condition. The last condition is given by the membrane and bending equilibrium equations of the interphases modeled as Kirchhoff plates. Numerical results that demonstrate the validity and efficiency of the formulation are presented for the case of a stack of silicon thin films embedded in epoxy.

Keyword: anisotropic elasticity, Fourier transform, Green's function, interface, interphase, Kirchhoff plate, membrane, multilayers, Stroh formalism.

1 Introduction

A special Green's function for multilayered anisotropic and linearly elastic solids with interphases exhibiting membrane and flexural rigidities is derived by applying the Stroh formalism and two-dimensional Fourier transforms (Ting, 1996). The Green's function satisfies the surface boundary condition, the interfacial displacement continuity condition and the interfacial traction discontinuity condition. The last condition is given by the equilibrium equations of the interphases treated as linear membranes and Kirchhoff plates in the in-plane and the out-of-plane deformation modes, respectively. This Green's function is applicable to a planar multilayer system where the interphases are thin but stiff compared to the matrix layers and thus are suitably modeled as Kirchhoff plates (Cao, Zhang and Cross, 1993; Benveniste, 2006; Benveniste and Miloh, 2001; Yoon, Lee, Lee, Koh, Kim and Lee, 2006).

The present work is an advance over the earlier developed Green's functions for generally anisotropic planar bimaterials, trimaterials and multilayers without interphase at the interfaces (Pan and Yuan, 2000; Tewary, Wagoner and Hirth, 1989; Yang and Pan, 2002a,b; Yang and Tewery, 2006; Yuan, Yang and Yang, 2003). Those Green's functions were derived by applying the generalized Stroh formalism and two-dimensional Fourier transforms (Ting, 1996). They have been applied to solving several engineering problems, including quantum dots (Yang and Pan, 2003), bolted joints (Yang, Pan and Yuan, 2003), and cracks (Yang, 2002) in composite laminates/multilayers. The special Green's functions have been found to be very useful in solving these engineering problems because their application minimizes the required computational effort. Furthermore, the solutions are accurate due to the analytical or semi-analytical nature of the Green's functions. This advantage is particularly attractive in dealing with problems with singularities such as cracks, interfacial free-edges, dislocations, steps and point defects. The Green's function as derived in the present paper offers the same advantage in application to problems dealing with

[1] Contribution of the National Institute of Standards and Technology, an agency of the US government; not subject to copyright.

[2] Department of Mechanical and Aerospace Engineering, Florida Institute of Technology, Melbourne, FL 32901

[3] Materials Reliability Division, National Institute of Standards and Technology, Boulder, CO 80305

modern advanced materials consisting of multilayers exhibiting finite interfacial membrane and flexural rigidities. It may also be applied to set up a continuum base for Green's function-based multiscale modeling (Tewary and Read, 2004; Yang and Tewary, 2007) of such multilayered nanomaterials.

In Sec. 2, the Green's function problem of a multilayered anisotropic and linearly elastic solid with interphases exhibiting membrane and flexural rigidities is formulated. In Sec. 3, the solution procedure is described. In Sec. 4, numerical results for the case of silicon films embedded in epoxy are presented that demonstrate the validity and efficiency of the present formulation. In Sec. 5, conclusions are drawn.

2 Problem Formulation

Consider a laterally infinite solid made of M planar layers of generally different materials, as shown in Fig. 1. A Cartesian coordinate system (x_1, x_2, x_3) is attached to the system, with the x_3-axis perpendicular to the surfaces and interfaces. The materials within each layer are homogeneous, generally anisotropic, and linearly elastic. The layers are perfectly bonded through interphases that exhibit membrane and flexural rigidities. Equivalently, the system may be viewed as a solid with embedded parallel plates with membrane and flexural rigidities and of generally distinct materials buffering between adjacent plates.

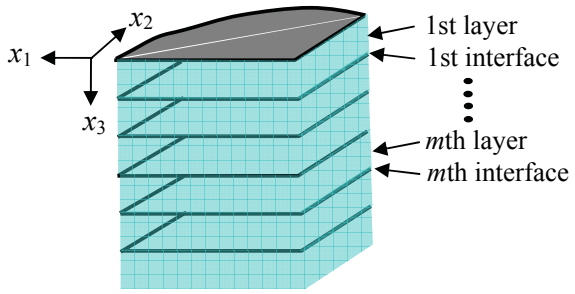

Figure 1: A multilayered solid with interfaces exhibiting membrane and flexural rigidities.

Hooke's law for each layer material is given by

$$\sigma_{ij} = C_{ijkl}\varepsilon_{kl}, \tag{1}$$

where σ is the stress tensor, ε is the strain tensor, defined by $\varepsilon_{kl} = \frac{1}{2}(u_{k,l} + u_{l,k})$, and C_{ijkl} is the elastic stiffness matrix. In the definition of strain ε, $\mathbf{u}$ is the displacement, and the subscript prime denotes the partial differentiation with respect to the index that follows. For generally anisotropic elastic material, C_{ijkl} consists of 21 independent elements. The standard notation system is used in the text. All Latin subscript indices range from 1 to 3. Later Greek subscript indices range from 1 to 2. A bold-faced symbol for a tensor implies that its indices range from 1 to 3. Repeated indices indicate the convention of summation.

Across the interphases, which are modeled as plates of trivial thickness but exhibiting membrane and flexural rigidities, the traction is discontinuous. Meanwhile, the displacement is continuous. The interfacial displacement continuity condition is given by

$$\mathbf{u}_m = \mathbf{u}_{m+1} at x_3 = h_m, \tag{2}$$

where h_m is the vertical level of the mth interface between the mth and (m+1)th layers. The interfacial traction discontinuity condition is given by (Timoshenko and Woinowsky-Krieger, 1959)

$$(\boldsymbol{\sigma}_{m+1} - \boldsymbol{\sigma}_m)\mathbf{n} = \mathbf{F}_m\mathbf{u}_m \text{ at } x_3 = h_m, \tag{3}$$

where $\mathbf{n}$ = (0, 0, 1), and differential operator $\mathbf{F}$ is given by

$$\mathbf{F} = \begin{bmatrix} -(E_{11}\frac{\partial^2}{\partial x^2} + E_{66}\frac{\partial^2}{\partial y^2}) & -(E_{12}+E_{66})\frac{\partial^2}{\partial x \partial y} & 0 \\ -(E_{21}+E_{66})\frac{\partial^2}{\partial x \partial y} & -(E_{66}\frac{\partial^2}{\partial x^2} + E_{22}\frac{\partial^2}{\partial y^2}) & 0 \\ 0 & 0 & D_x\frac{\partial^4}{\partial x^4} + 2H\frac{\partial^4}{\partial x^2 \partial y^2} + D_y\frac{\partial^4}{\partial y^4} \end{bmatrix} \tag{4}$$

The interphase membrane behavior, given by the first two rows in Eq. (4), is assumed to be linear and generally anisotropic. The membrane stiffness constants (E_{11}, E_{12}, E_{22}, E_{66}) are related to the elastic constants of the interphase material (assumed to be homogeneous) by $\mathbf{E} = \mathbf{C}h$, where h

is the plate thickness, and **C** is the reduced form of C_{ijkl} in Eq. (1). The initial stress in all the interphases is assumed to be null. The interphase bending behavior is assumed to be of the Kirchhoff type and generally anisotropic. The flexural rigidity components (D_x, D_y, H) are related to the elastic constants and thickness of the interphase by

$$D_x = \frac{C_{11}h^3}{12}, \quad H = \frac{(C_{12}+C_{66})h^3}{12}, \quad D_y = \frac{C_{22}h^3}{12}. \tag{5}$$

The above formulation is applicable to a material system of trivial interphase thickness but significant interphase moduli compared to the layer properties.

The multilayered solid shown in Fig. 1 is subjected to a point force **f** applied at source point **X**. The differential equilibrium equations within the buffering material are given by

$$\sigma_{ij,j} + f_i \delta(\mathbf{x}-\mathbf{X}) = 0, \tag{6}$$

where δ(**x**-**X**) is the Dirac delta function. Substituting Eq. (1) into Eq. (6) and realizing the symmetry of the elastic stiffness matrix **C** yield

$$C_{ijkl}u_{k,lj} + f_i \delta(\mathbf{x}-\mathbf{X}) = 0. \tag{7}$$

The equilibrium condition of the interphase material was previously given in Eqs. (3) and (4).

A homogeneous boundary condition consisting of either zero displacement or zero traction in each component is applied upon the top and bottom surfaces of the multilayered solid (except for the case of zero normal traction components on both surfaces, which would result in indefinite rigid-body motion). In addition, the radiation condition is imposed, by which the displacement field as well as the stress field diminishes at infinity. The solution to Eq. (7), together with the interfacial conditions and the surface and radiation conditions, is the Green's function of the material system. The Green's function can be directly applied to solve defect problems within this system. It can also be applied to develop a numerical boundary element method to solve problems with only discretization upon areas where those conditions are altered.

3 Green's Function Solution

In this section, the general solution to Eq. (7) is first derived for each homogeneous layer by applying the generalized Stroh formalism (Ting, 1996). The Green's function for multilayers with interfacial rigidities is then derived by imposing the surface boundary condition, the interfacial conditions (Eqs. (2) and (3)), and the remote radiation condition.

To start with, the following two-dimensional Fourier transform (y_1, y_2) is applied to the in-plane coordinates (x_1, x_2) of a field quantity, for instance, u_i, as

$$\tilde{u}_i(y_1,y_2,x_3) = \int_{-\infty}^{\infty}\int_{-\infty}^{\infty} u_i(x_1,x_2,x_3)\, e^{ix_\alpha y_\alpha} dx_1 dx_2, \tag{8}$$

where e stands for the exponential function, and i in the exponent denotes $\sqrt{-1}$. Thus, in the transform domain, the governing equation (7) becomes

$$C_{i3k3}\tilde{u}_{k,33} - i(C_{i\alpha k3}+C_{i3k\alpha})y_\alpha \tilde{u}_{k,3} - C_{i\alpha k\beta}y_\alpha y_\beta \tilde{u}_k = -f_i e^{iX_\alpha y_\alpha}\delta(x_3 - X_3). \tag{9}$$

Solving this ordinary differential equation in terms of x_3 with **f** being a unit force in the Ith direction yields the general expression for the transform-domain Green's function in the ith component, $\tilde{u}^*_{Ii}$, as

$$\tilde{\mathbf{u}}^*_m(x_3) = e^{iy_\alpha X_\alpha}\Big[\tilde{\mathbf{u}}^{*(s)}_m(x_3) + i\eta^{-1}\Big(\overline{\mathbf{A}}_m\Big\langle e^{-i\overline{\mathbf{p}}_m\eta(x_3-h_{m-1})}\Big\rangle \mathbf{V}_m + \mathbf{A}_m\Big\langle e^{-i\mathbf{p}_m\eta(x_3-h_m)}\Big\rangle \mathbf{W}_m\Big)\Big], \tag{10}$$

where the subscript m indicates the quantities are associated to the mth layer where the field point **x** resides; $\tilde{\mathbf{u}}^*_m$ is a function of y_1, y_2 and **X** as well as x_3; $\tilde{\mathbf{u}}^{*(s)}_m$, a seed solution, is a given function of y_1, y_2 and **X** as well as x_3; and $\mathbf{V}_m$ and $\mathbf{W}_m$ are a pair of unknown functions to be determined by the boundary and interfacial conditions. The dummy arguments in these functions, which are not relevant directly to the following imposition of boundary and interfacial conditions, are omitted for simplicity. In addition, the overbar denotes

the complex conjugate, $(\eta,\ \theta)$ are the polar coordinates related to (y_1, y_2) by $y_1 = \eta\cos\theta$ and $y_2 = \eta\sin\theta$, $\mathbf{p}$ and $\mathbf{A}$ as functions of θ and C_{ijkl} are the eigenvalues and eigenvectors of the generalized Stroh eigenproblem (Ting, 1996), and

$$\left\langle e^{-i\mathbf{p}\eta x_3}\right\rangle \equiv diag\left[e^{-ip_1\eta x_3}, e^{-ip_2\eta x_3}, e^{-ip_3\eta x_3}\right]. \tag{11}$$

Note that Eq. (10) satisfies the aforementioned radiation condition as long as the special solution, $\tilde{\mathbf{u}}_m^{*(s)}$, satisfies it. It is also noted that a superscript asterisk has been attached to the displacement to dictate that it is the general/fundamental solution. From the fundamental solution, the Green's function due to a point force in an arbitrary direction can be derived. One may refer to Ting (1996) for definition of the characteristic equation and the matrix $\mathbf{A}$ and derived matrices $\mathbf{B}$ and $\mathbf{C}$ in the following. These details are omitted here for the sake of brevity.

By applying the constitutive law in Eq. (1), the transform-domain in-plane stress components $\tilde{\mathbf{s}}^* \equiv (\tilde{\sigma}^*_{I11}, \tilde{\sigma}^*_{I12}, \tilde{\sigma}^*_{I22})$ and out-of-plane stress components $\tilde{\mathbf{t}}^* \equiv (\tilde{\sigma}^*_{I13}, \tilde{\sigma}^*_{I23}, \tilde{\sigma}^*_{I33})$ can be derived from the Green's function $\tilde{\mathbf{u}}^*_m$ in Eq. (10) as

$$\begin{aligned}\tilde{\mathbf{t}}^*_m(x_3) = e^{iy_\alpha X_\alpha}\Big[&\tilde{\mathbf{t}}^{*(s)}_m(x_3)\\ &+\left(\overline{\mathbf{B}}_m\left\langle e^{-i\overline{\mathbf{p}}_m\eta(x_3-h_{m-1})}\right\rangle\mathbf{V}_m\right.\\ &\left.+\mathbf{B}_m\left\langle e^{-i\mathbf{p}_m\eta(x_3-h_m)}\right\rangle\mathbf{W}_m\right)\Big],\end{aligned} \tag{12}$$

$$\begin{aligned}\tilde{\mathbf{s}}^*_m(x_3) = e^{iy_\alpha X_\alpha}\Big[&\tilde{\mathbf{s}}^{*(s)}_m(x_3)\\ &+\left(\overline{\mathbf{C}}_m\left\langle e^{-i\overline{\mathbf{p}}_m\eta(x_3-h_{m-1})}\right\rangle\mathbf{V}_m\right.\\ &\left.+\mathbf{C}_m\left\langle e^{-i\mathbf{p}_m\eta(x_3-h_m)}\right\rangle\mathbf{W}_m\right)\Big],\end{aligned} \tag{13}$$

where $\tilde{\mathbf{t}}^{*(s)}_m$ and $\tilde{\mathbf{s}}^{*(s)}_m$ are derived from $\tilde{\mathbf{u}}^{*(s)}_m$ in the same way as $\tilde{\mathbf{t}}^*_m$ and $\tilde{\mathbf{s}}^*_m$ from $\tilde{\mathbf{u}}^*_m$, and matrix $\mathbf{B}$ and $\mathbf{C}$ are derived from $\mathbf{A}$ and $\mathbf{p}$. Note that the matrix $\mathbf{C}$ here is different from the fourth-rank elastic stiffness tensor C_{ijkl} or its reduced matrix form.

The interfacial conditions, Eqs. (2) and (3), are given in the transform domain as

$$\tilde{\mathbf{u}}^*_m = \tilde{\mathbf{u}}^*_{m+1} \text{ at } x_3 = h_m. \tag{14}$$

The corresponding interfacial traction discontinuity condition is given by

$$(\tilde{\boldsymbol{\sigma}}^*_{m+1} - \tilde{\boldsymbol{\sigma}}^*_m)\mathbf{n} = \tilde{\mathbf{F}}_m\tilde{\mathbf{u}}^*_m \text{ at } x_3 = h_m, \tag{15}$$

$$\tilde{\mathbf{F}} = \begin{bmatrix} E_{11}y_1^2 + E_{66}y_2^2 & (E_{12}+E_{66})y_1y_2 & 0\\ (E_{21}+E_{66})y_1y_2 & E_{66}y_1^2 + E_{22}y_2^2 & 0\\ 0 & 0 & 0\\ 0 & 0 & D_xy_1^4 + 2Hy_1^2y_2^2 + D_yy_2^4 \end{bmatrix} \tag{16}$$

Substituting Eqs. (10) and (12) in Eqs. (14) and (15) together with the boundary condition results in a system of $2M$ algebraic equations. This system of equations can be solved to determine the $2M$ unknown vectors $\mathbf{V}_m$ and $\mathbf{W}_m$ (for $m = 1,\ldots,M$) for all the layers, which are essentially the solution to the Green's function in the transform domain (Yang and Pan, 2002; Yuan, Yang and Yang, 2003).

Once the transform-domain solution is found, the Green's function in the physical domain can be derived by the Fourier inverse transform. For instance, the physical-domain Green's function of displacement can be expressed as

$$u_i(x_1,x_2,x_3) = \frac{1}{(2\pi)^2}\int_{-\infty}^{\infty}\int_{-\infty}^{\infty}\tilde{u}_i(y_1,y_2,x_3)\,e^{-ix_\alpha y_\alpha}dy_1dy_2. \tag{17}$$

Evaluation efficiency of the Green's function would depend strongly on the chosen seed solution $\tilde{\mathbf{u}}^{*(s)}_m$, as shown in the case of multilayers without interfacial rigidities (Yang and Pan, 2002). The seed solution should be chosen such that it takes a large part in the total function and that its evaluation is more efficient than the evaluation of the two-dimensional integral in Eq. (17). In the present work, the following infinite-space

Green's function is used for $\tilde{\mathbf{u}}_m^{*(s)}$:

$$\tilde{\mathbf{u}}^{*(\infty)}(x_3) = \begin{cases} i\eta^{-1}\mathbf{A}\left\langle e^{-i\mathbf{p}\eta(x_3-X_3)}\right\rangle \mathbf{A}^{-1}\left(\mathbf{M}-\overline{\mathbf{M}}\right)^{-1}, \\ \qquad\qquad x_3 < X_3 \\ i\eta^{-1}\overline{\mathbf{A}}\left\langle e^{-i\overline{\mathbf{p}}\eta(x_3-X_3)}\right\rangle \overline{\mathbf{A}}^{-1}\left(\mathbf{M}-\overline{\mathbf{M}}\right)^{-1}, \\ \qquad\qquad x_3 > X_3 \end{cases}, \tag{18}$$

$$\tilde{\mathbf{t}}^{*(\infty)}(x_3) = \begin{cases} \mathbf{B}\left\langle e^{-i\mathbf{p}\eta(x_3-X_3)}\right\rangle \mathbf{A}^{-1}\left(\mathbf{M}-\overline{\mathbf{M}}\right)^{-1}, & x_3 < X_3 \\ \overline{\mathbf{B}}\left\langle e^{-i\overline{\mathbf{p}}\eta(x_3-X_3)}\right\rangle \overline{\mathbf{A}}^{-1}\left(\mathbf{M}-\overline{\mathbf{M}}\right)^{-1}, & x_3 > X_3 \end{cases}. \tag{19}$$

The physical-domain counterparts of Eqs. (18) and (19) can be analytically evaluated; see refs. (Wang, 1997; Pan and Tonon, 2000; Yang, Pan and Tewary, 2004). The inverse transform of the remaining part due to the heterogeneity of the material system, including the layer heterogeneity and the interphase heterogeneity, is carried out numerically by a standard adaptive quadrature scheme.

4 Numerical Results

In this section, the point force solution (i.e., Green's function) is presented for a system of a stack of parallel Si(001) films embedded in a semi-infinite epoxy matrix. Alternatively, the material system is viewed as multiple epoxy layers bonded/separated by parallel Si films. The Young's modulus and Poisson's ratio of the isotropic epoxy are 2.6 GPa and 0.35, respectively. The elastic constants of the cubic Si films are C_{11} = 165.8 GPa,C_{12} = 63.9 GPa,C_{44} = 79.6 GPa. Their moduli are a couple of orders in magnitude different. The full elastic stiffness matrices can be constructed based on these constants as described in Ting (1996). The film spacing is indicated by s, and the film thickness h is set to be s/10. The films are modeled as plates (of trivial thickness) and thus the previous formulation can apply. In the following calculation, a system of 50 Si films is considered. The first Si film is buried at a depth of s from the surface.

Such a material consisting of a compliant matrix embedded with stiff but thin films has been a long-standing difficulty/challenge to numerical modeling. The difficulty lies in that while the film restraining effect on in-plane deformation is significant due to the stiff moduli, its effect on out-of-plane deflection may be small due to its cubic power dependence on thickness compared to the linear dependence in the former. The thin film may bend fairly freely but be severely restrained from in-plane deformation. An often adopted approach to such films as being unstretchable can account for the in-plane restraining but not the flexural bending effect.

Before moving on to the discussion of the numerical results, it may be worth mentioning that the elastic constants C_{ij} of the isotropic epoxy is artificially skewed a little from the full isotropy. This is necessarily done in order to apply the previous formulation of generally anisotropic elasticity to this case of isotropy. Otherwise, special treatment would be needed for this degenerated case (Ting, 1996), which is not attempted in the present work. It was checked that the extent of anisotropy introduced affects little the numerical results.

For the purpose of demonstration, a point force of one unit of $E_0 s^2$, where E_0 = 1 GPa, is applied on the otherwise traction-free top surface at (x_1=0, x_2=0, x_3=0). The force is directed along either x_1 or x_3 axis. The resulting displacement and stress are evaluated along a line (x_1, x_2=0, x_3=s) on both sides of the first interphase. The numerical results (of nonzero components) are plotted in Figs. 2-5. The solutions in the absence of films are included for comparison. Figures 2 and 3 are for the case of a point force being applied along the x_1 axis. Figures 4 and 5 are for the case of a point force being applied along the x_3 axis.

From Figs. 2 and 4, it can be seen that the displacement is identical across the interphase plate, which is consistent with the interfacial displacement continuity condition (Eq. (2)) imposed in the formulation in Sec. 2. Meanwhile, from Figs. 3 and 5, it can be seen that all the stress components are discontinuous across the interfacial plate, as a result of the imposed interphase membrane and plate conditions (Eq. (3)). Recall that

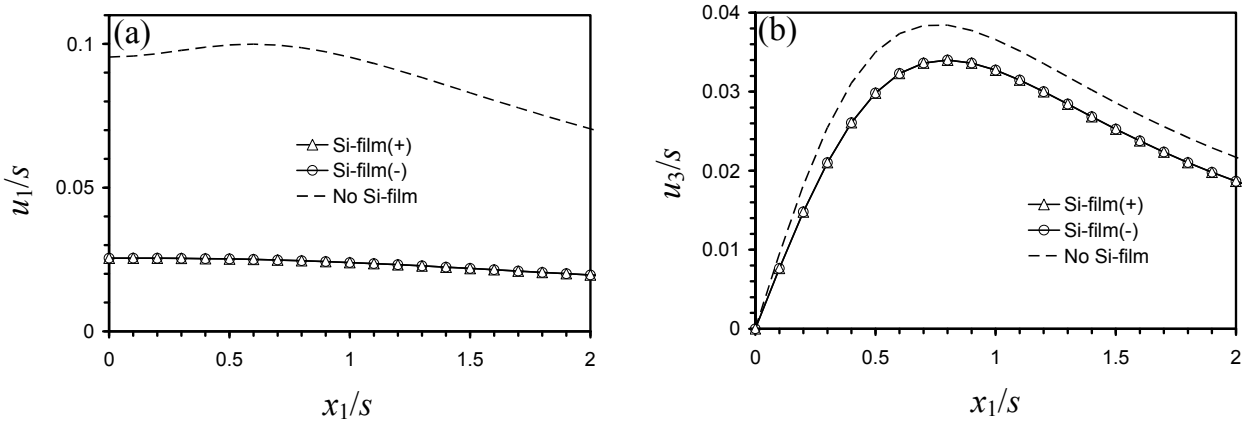

Figure 2: Variation of displacements along a line (x_1, 0, s) due to a unit point force applied along the x_1 axis at (0,0,0) on the top surface. The triangle symbol denotes a quantity on the near force side of an interface, while the circular symbol denotes the quantity on the other side of the interface. The dashed line denotes the solution in the absence of all films.

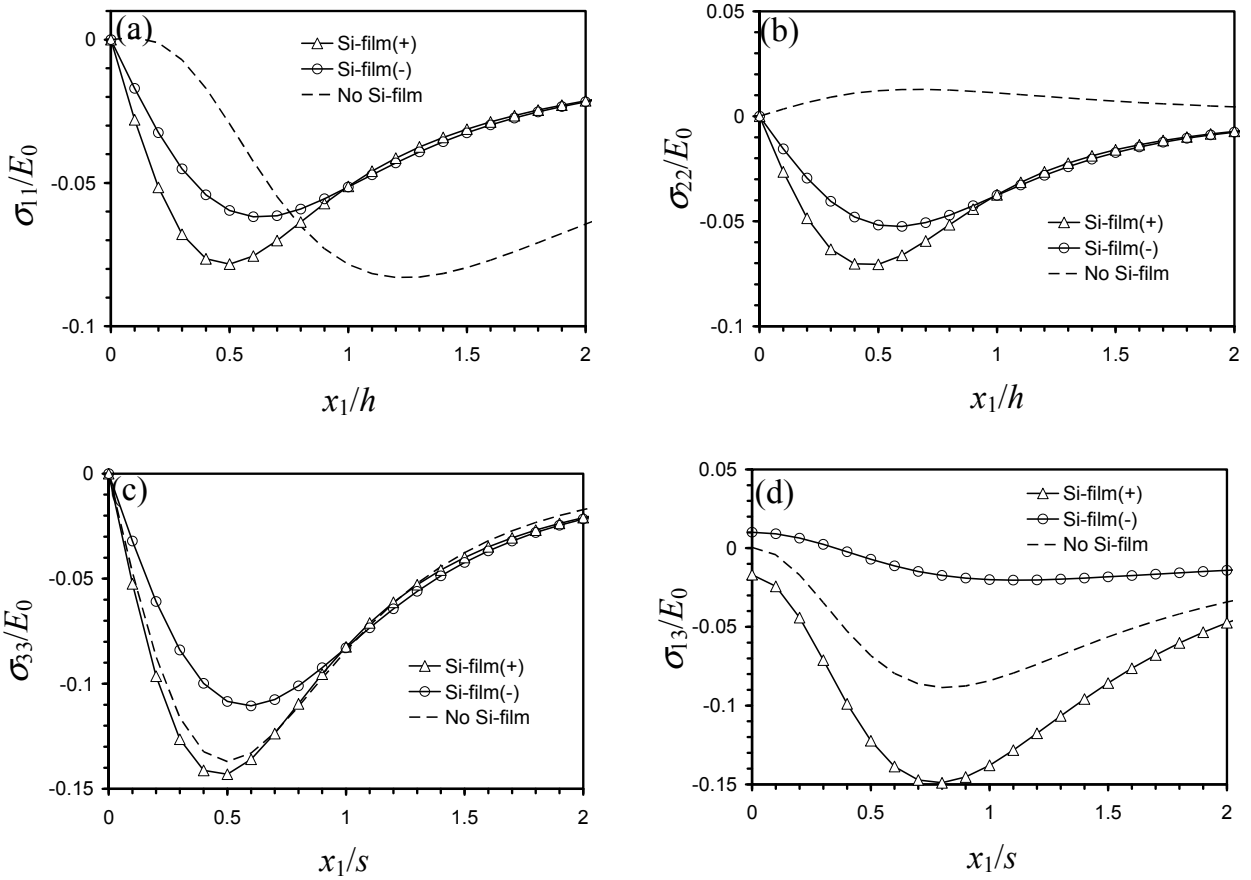

Figure 3: Variation of stresses along a line (x_1, 0, s) due to a unit point force applied along the x_1 axis at (0,0,0) on the top surface. The triangle symbol denotes a quantity on the near force side of an interface, while the circular symbol denotes the quantity on the other side of the interface. The dashed line denotes the solution in the absence of all films.

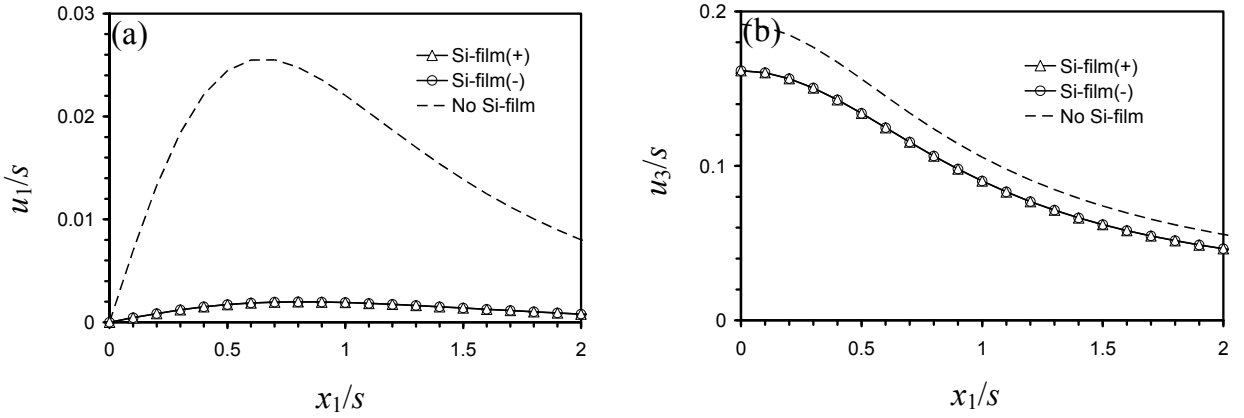

Figure 4: Variation of displacements along a line (x_1, 0, s) due to a unit point force applied along the x_3 axis at (0,0,0) on the top surface. The triangle symbol denotes a quantity on the near force side of an interface, while the circular symbol denotes the quantity on the other side of the interface. The dashed line denotes the solution in the absence of all films.

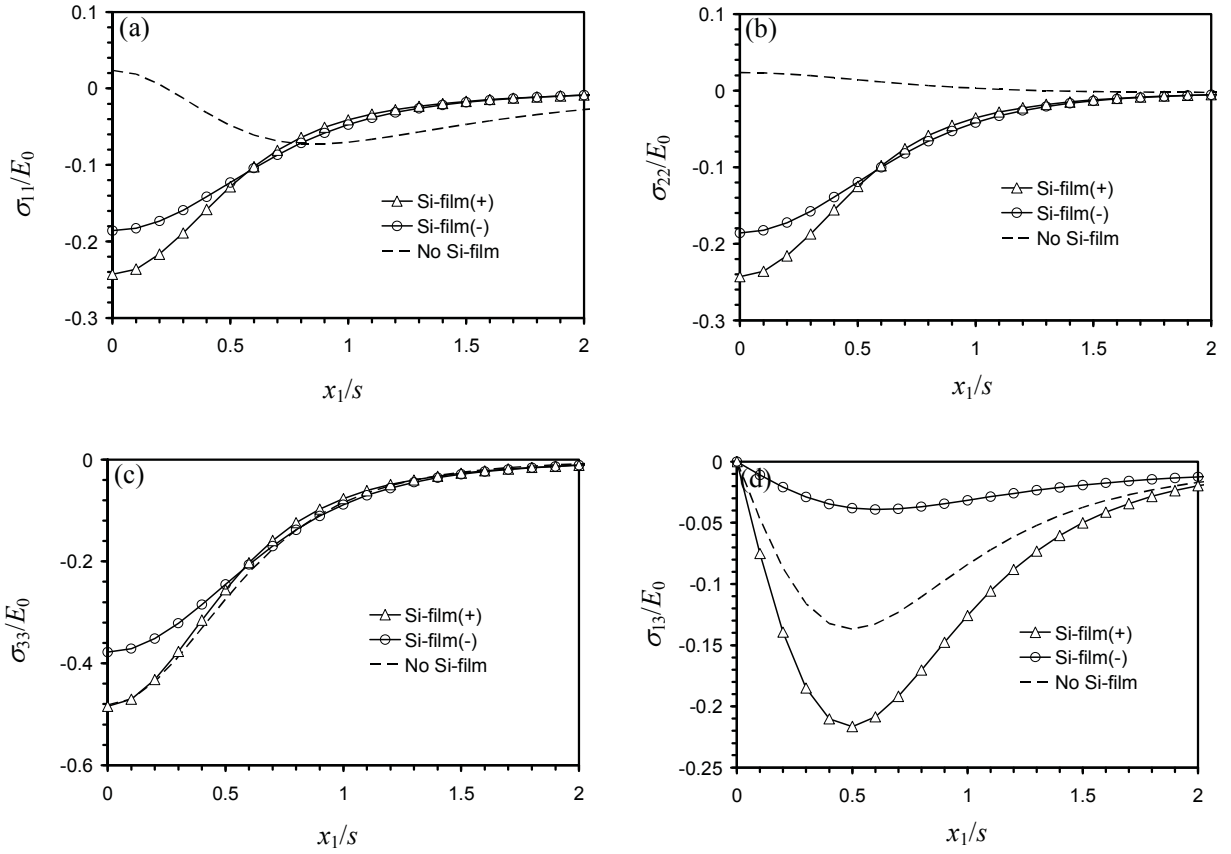

Figure 5: Variation of stresses along a line (x_1, 0, h) due to a unit point force applied along the x_3 axis at (0,0,0) on the top surface. The triangle symbol denotes a quantity on the near force side of an interface, while the circular symbol denotes the quantity on the other side of the interface. The dashed line denotes the solution in the absence of all films.

the Si film moduli are a couple of orders of magnitude greater than that of the epoxy. As can be seen by comparing of (a) and (b) for the lateral and normal displacement components, respectively, in both Figs. 2 and 4, the presence of the films effectively restrains the in-plane deformation. In contrast, its restraining effect against the out-of-plane deformation is much less effective due to the relatively small flexural rigidity of the Si-film which is proportional to the third power of film thickness. This result signifies the present approach to a solid with embedded relatively stiff but thin films, rather than assuming the films completely rigid.

5 Conclusions

A Green's function for a material system consisting of a linear elastic matrix material with embedded planar multilayers with interfacial membrane and flexural rigidities has been derived by applying the generalized Stroh formalism and two-dimensional Fourier transforms. The individual layers are modeled as generally anisotropic and linearly elastic. The interphase material is modeled as an anisotropic linear membrane with Kirchhoff-type bending characterisitcs. The Green's function satisfies the interfacial displacement continuity condition, the interfacial membrane and bending equilibrium equations, and a homogeneous boundary condition on the top and bottom surfaces. It can be applied to accurately model a stack of plates or thin films embedded in a relatively soft matrix, and layered nanomaterials with high interface-to-volume ratio. It can also be applied to model graphite, where the individual graphene sheets are treated as plates and the Van der Waals interaction is treated as a buffering material between the plates. In particular, the case of a stack of parallel Si films in an epoxy matrix is numerically examined. The high in-plane membrane rigidity but finite flexural rigidity of the films whose elastic constants are about two orders of magnitude greater than that of the epoxy matrix are accurately represented. The numerical results are consistent with the imposed conditions, demonstrating the validity and efficiency of the present formulation.

Acknowledgement: The authors thank Prof. Walter Gerstle for his comments on the paper and useful suggestions. BY acknowledges the financial support from the National Science Foundation (CMMI-0723486) and a summer support from the National Institute of Standards and Technology that initiated the study.

Reference

Benveniste, Y. (2006): A general interface model for a three-dimensional curved thin anisotropic interphase between two anisotropic media. *Journal of the Mechanics and Physics of Solids*, vol. 54, pp. 708-734.

Benveniste, Y.; Miloh, T. (2001): Imperfect soft and stiff interfaces in two-dimensional elasticity. *Mechanics of Materials*, vol. 33, pp. 309-323.

Cao, W.; Zhang, Q. M.; Cross, L. E. (1993): Theoretical study on the static performance of piezoelectric ceramic-polymer composites with 2-2 connectivity. *IEEE Transactions on Ultrasonics, Ferroelectrics and Frequency Control,* vol. 40, pp. 103-109.

Pan, E.; Tonon, F. (2000): Three-dimensional Green's functions in anisotropic piezoelectric solids. *International Journal of Solids and Structures*, vol. 37, pp. 943-958.

Pan, E.; Yuan, F. G. (2000): Three-dimensional Green's functions in anisotropic biomaterials. *International Journal of Solids and Structures*, vol. 37, pp. 5329-5351.

Tewary; V. K.; Read D. T. (2004): Integrated Green's function molecular dynamics method for multiscale modeling of nanostructures: Application to Au nanoisland in Cu. *CMES: Computer Modeling in Engineering & Sciences,* vol. 6, pp. 359-372.

Tewary, V. K.; Wagoner R. H.; Hirth, J. P. (1989): Elastic Green's function for a composite solid with a planar interface. *Journal of Materials Research,* vol 4, pp. 113-123.

Timoshenko, S.; Woinowsky-Krieger, S. (1959): Theory of Plates and Shells, McGraw-Hill Book Company, New York.

Ting, T. C. T. (1996): Anisotropic Elasticity, Ox-

ford University Press, Oxford.

Wang, C. Y. (1997): Elastic fields produced by a point source in solids of general anisotropy. *Journal of Engineering Mathematics*, vol. 32, pp. 41-52.

Yang, B. (2002): Examination of free-edge delamination around an open hole in composite laminates. *International Journal of Fracture,* vol. 115, pp. 173-191.

Yang, B.; Pan, E. (2002a): Three-dimensional Green's functions in anisotropic trimaterials. *International Journal of Solids and Structures,* vol. 39, pp. 2235-2255.

Yang, B.; Pan, E. (2002b): Efficient evaluation of three-dimensional Green's functions in anisotropic elastostatic multilayered composites. *Engineering Analysis with Boundary Elements*, vol. 26, pp. 355-366.

Yang, B.; Pan, E. (2003): Elastic fields of quantum dots in multilayered semiconductors: A novel Green's function method. *ASME Journal of Applied Mechanics*, vol. 70, pp. 161-168.

Yang, B.; Pan, E.; Tewary, V. K. (2004): Three-dimensional Green's function of steady-state motion in anisotropic half-space and biomaterials. *Engineering Analysis with Boundary Elements*, vol. 28, pp. 1069-1082.

Yang, B.; Pan, E.; Yuan, F. G. (2003): Three-dimensional stress analysis of composite laminates with an elastically fastened hole. *International Journal of Solids and Structures*, vol. 40, pp. 2017-2035.

Yang, B.; Tewary, V. K. (2006): Efficient Green's function method of line and surface defects in multilayered elastic and piezoelectric materials. *CMES: Computer Modeling in Engineering & Sciences*, vol. 15, pp. 165-178.

Yang, B.; Tewary, V. K. (2007): Multiscale modeling of point defects in Si-Ge(001) quantum wells. *Physical Review B,* vol. 75, pp. 144103-1-11.

Yoon, C.-B.; Lee, S.-H.; Lee, S.-M.; Koh, Y.-H.; Kim, H.-E.; Lee, K.-W. (2006): Piezoelectric multilayer ceramic/polymer composite transducer with 2-2 connectivity. *Journal of the American Ceramic Society,* vol. 89, pp. 2509-2513.

Yuan, F. G.; Yang, S.; Yang, B. (2003): Three-dimensional Green's functions for composite laminates. *International Journal of Solids and Structures*, vol. 40, pp. 331-342.